

Fast, sensitive laser deflection system suitable for transient plasma analysis

C. L. Enloe, R. M. Gilgenbach, and J. S. Meachum

*Intense Energy Beam Interaction Laboratory, Department of Nuclear Engineering,
The University of Michigan, Ann Arbor, Michigan 48109-2104*

(Received 11 May 1987; accepted for publication 26 May 1987)

A laser deflection measurement system has been developed which is both fast ($\tau \approx 20$ ns) and sensitive ($\delta\phi \approx 0.5 \mu\text{rad}$). This diagnostic is capable of sensing and discriminating between electrons and neutral particles in a multicomponent plasma, and yields quantitative results. The technique allows continuous measurements in time. Construction is inexpensive and simple to field. This system is, therefore, highly competitive with traditional techniques in diagnosing the development of transient plasmas.

INTRODUCTION

Investigation of the time evolution of the plasma produced by the interaction of a high-power laser with a target is an example of a situation in which a fast, versatile probe of plasma density is desirable.¹ Such a plasma is short lived, since the plasma is expanding with a velocity on the order of $10 \text{ cm}/\mu\text{s}$, and composed of different components. In particular, at early times a dense plasma exists, whereas at late times the presence of a neutral component is significant.

The common technique of pulsed laser schlieren photography^{2,3} is inadequate to diagnose the temporal evolution of such a plasma in a single shot. Although fast (20-ns) "shuttering times" can be obtained by employing a Q -switched ruby laser, many identical plasma shots are required, varying the timing of the probe laser, to observe the plasma evolve in time. In many cases, difficulties arise because of the neutral component, since the presence of a plasma is a negative perturbation in the index of refraction while the presence of neutral particles is a positive perturbation. If a pinhole is used as a spatial filter in a schlieren system, the technique can simultaneously detect both plasmas and neutrals, but cannot distinguish between them. If a knife edge is used as a spatial filter, the technique can distinguish between the two but cannot detect them simultaneously. Further, it is difficult to obtain quantitative results from schlieren photography.⁴ Applying the technique of holographic interferometry⁵ eliminates these difficulties, but at the expense of a large increase in cost and complexity, since not only are the laser optics required to make the hologram more complex, but the hologram must be reconstructed in order to interpret the results.

Diagnosing density by measuring the deflection of a laser beam^{6,7} is an analogous technique to schlieren photography, in that both techniques are sensitive to index of refraction gradients. The technique has been successfully applied to a number of fields⁷; the chief impediment to its application to transient plasmas has been one of speed. In this article, we present a laser deflection system capable of detecting deflections of $0.5 \mu\text{rad}$ on a time scale of 20 ns. Hence, its speed is comparable to Q -switched ruby laser schlieren, while its sensitivity is over two orders of magnitude greater. It is inher-

ently quantitative, while at the same time being much simpler and less expensive to implement than a ruby laser and associated optics.

I. LASER DEFLECTION TECHNIQUE

Figure 1 illustrates the laser deflection technique applied to a laser-produced plasma. The target material is produced by focusing the output of a Q -switched ruby laser on a graphite surface. A 5-mW He-Ne probe laser (Jodon Laser model HN-2SHP) is deflected by index of refraction gradients as it passes through the laser-produced plasma. The angular deflection is given by⁶

$$\delta\phi = \frac{1}{\bar{n}_0} \left| \int_{\text{path}} ds \nabla_{\perp} \bar{n} \right| = \frac{D \langle \nabla_{\perp} \bar{n} \rangle}{\bar{n}_0}, \quad (1)$$

where \bar{n} is the index of refraction, \bar{n}_0 is the unperturbed index of refraction (approximately equal to 1), $\nabla_{\perp} \bar{n}$ is the gradient in the index of refraction perpendicular to the path of the beam, D is the thickness of the plasma, and $\langle \rangle$ indicates a line average taken over the path of the probe laser in the plasma. Since deflections are small, this average is taken over the straightline unperturbed path. The deflection of the

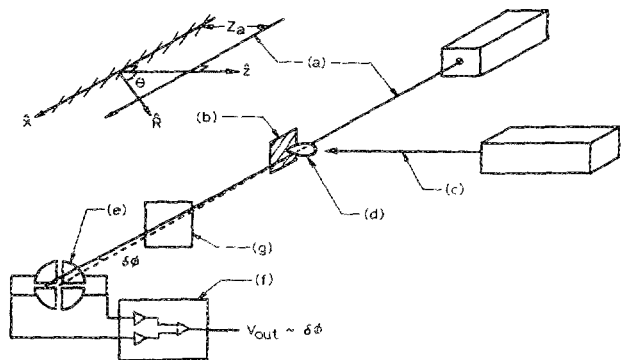


FIG. 1. Experimental configuration and coordinate system used for analysis. (a) He-Ne probe laser beam. (b) Carbon target. (c) Ruby laser beam. (d) Laser-produced plasma. (e) Quadrant detector. (f) Differencing and amplifying circuitry. (g) He-Ne laser line filter.

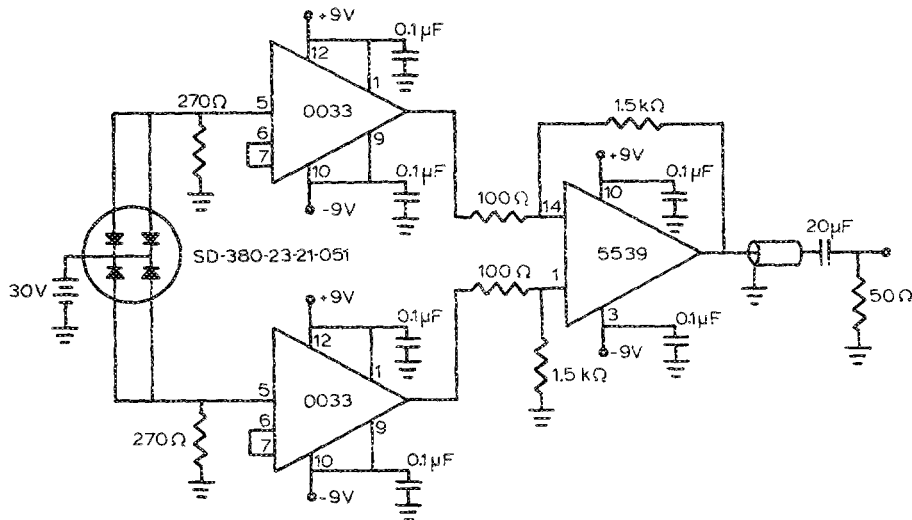


FIG. 2. Laser position sensor circuit, rise time $\tau = 20$ ns, sensitivity 1.25 mV/ μ m for a 0.5 -mW He-Ne laser.

beam is detected by a position sensor, specifically a quadrant detector (Silicon Detector Corporation model SD-380-23-21-051), chosen for its fast response time. The sensor and its associated electronics are located a distance L from the plasma. Although the design of the detector circuit is inherently noise resistant, a He-Ne laser line filter is used in front of the position sensor to maximize detector sensitivity by eliminating background light. The output of the detector is proportional to the deflection, $V(t) = C\delta\phi(t)$, where the constant C is readily calibrated.

For plasmas, the change in index of refraction $\delta\tilde{n}$ is proportional to the electron density n_e , and is given by²

$$\delta\tilde{n} = -\left(\frac{e^2}{2\pi m f^2}\right) n_e = -K_p n_e, \quad (2)$$

where e is the electron charge, m is the electron mass, and f is the laser frequency, so that $K_p = 1.79 \times 10^{-22}$ cm³ for He-Ne laser light. For neutral particles, $\delta\tilde{n}$ is proportional to the neutral density n_n , and is given by⁸

$$\delta\tilde{n} = \left(\frac{\tilde{n}_0 - 1}{n_0}\right)_{STP} n_n = K_n n_n. \quad (3)$$

At STP, the neutral density $n_0 = 2.6868 \times 10^{19}$ cm⁻³ and $(\tilde{n}_0 - 1) = 2.76 \times 10^{-4}$ for He-Ne laser light, so that $K_n = 1.0272 \times 10^{-23}$ cm³.

The key to the performance of this system is the detector circuit, shown in Fig. 2. The quadrant detector is essentially four photodiodes on one substrate. Each pair of anodes on either side of the vertical midplane are connected, so that the detector is sensitive only to horizontal deflections of the probe laser. A bias voltage of 30 V applied to the common connection reduces the output capacitance, and hence the response time, of the detector. Voltage is developed across a 270- Ω resistor on each side. This resistance value was chosen to optimize the gain-bandwidth product of the system. The signal from each side is buffered and passed on to a $15\times$ -gain differential amplifier. Since a differential configuration is used, the detector is insensitive to common-mode noise such as variations in probe laser power. The amplifier is capable of driving a 50- Ω load to approximately ± 1 V. A high-pass

filter is used to eliminate the effects of mechanical vibrations (≤ 20 Hz) from the output.

The sensitivity of the system is a function of laser power and spot size. It generally increases as the moment arm L ; however, for large L the effect of beam divergence is large and the advantage of the long arm diminishes. For the laser employed, $L \approx 3$ m appears to be optimum, yielding $dV/d\phi = 4.2$ mV/ μ rad. Since the output noise level is approximately 2 mV, the resolution of the system is approximately 0.5 μ rad. For comparison, consider a typical schlieren system with a 500-mm focal length lens and a 100- μ m pinhole. If we assume that the minimum detectable deflection is equivalent to a one- f -stop change in density on the film, then the resolution of this schlieren system is approximately 100 μ rad. Therefore, the laser deflection technique offers higher resolution than the schlieren technique by over two orders of magnitude.

The time response of the system was tested by masking one side of the detector at a time and using the detector to view a highly attenuated ruby laser pulse, comparing the output to that of a fast (2-ns rise time) PIN diode. The results are shown in Fig. 3. Using the formula for the addition of rise times,⁹

$$\tau_{\text{net}} = \left(\sum_n \tau_n^2\right)^{1/2} = (\tau_{\text{laser}}^2 + \tau_{\text{circuit}}^2)^{1/2}, \quad (4)$$

we find that the response time of the circuit itself is approximately 20 ns. Differences in light path lengths to the detec-

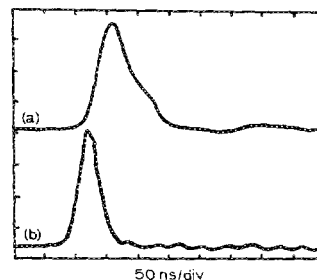


FIG. 3. (a) Response of one side of the position sensor to a ruby laser pulse, 50 mV/div, compared to (b) response of a fast PIN diode to the same pulse, 100 mV/div. The response of the other side of the position sensor is opposite in polarity, due to the differential configuration of the circuit.

tors, cable lengths from the detectors to the oscilloscope, and relative timing between the oscilloscope channels account for less than 1 ns in the timing difference between the signals. A fixed circuit delay of approximately 30 ns is, therefore, apparent.

II. APPLYING THE TECHNIQUE TO A MULTICOMPONENT PLASMA

Since the laser deflection technique yields information about density gradients, for any arbitrary configuration, it is possible to probe the plasma at a number of positions over a number of shots and integrate dn/dx over space to obtain the density distribution. However, in many cases, it is possible to obtain density information on a single shot, if the density as a function of time can be cast in the form of

$$n(r, t) = Sf(r, t), \quad (5)$$

where n is the density as a function of space and time, S is a scaling factor, and f is a function which describes the shape of the density in space and time.¹⁰ For example, in the case of a laser-produced plasma, a self-similar expansion model¹¹ gives the form, applicable to each species,

$$n_j(R, \theta, t) = \frac{2N_{Tj} k_j^2}{\pi^{3/2} (v_{zj}^0 t)^3} \exp\left(-\frac{R^2}{(v_{zj}^0 t)^2}\right) \times [(k_j^2 - 1) \sin^2 \theta + 1], \quad (6)$$

where n_j is the density of the j th species, N_{Tj} is the total number of that species produced by the laser, v_{zj}^0 is the characteristic expansion velocity of that species normal to the target surface, and k_j is the ratio of parallel to perpendicular velocities for that species. Figure 1 illustrates the coordinate system. The characteristic expansion velocity is largely independent of the number of each species produced in a given pulse; therefore, N_T is the scaling factor, and the remainder of the expression describes the spatial and temporal shape of the plasma. For the plasma under consideration, k_p has been measured¹² and is equal to 2, while k_n is taken to be 1. Using the transformation applicable to this geometry,

$$\nabla_j \bar{n} = \hat{z} \frac{Z_a}{R} \frac{d\bar{n}}{dR}, \quad (7)$$

where Z_a is the distance from the laser to the target, Eq. (1) becomes

$$\delta\phi = 2Z_a \int_0^\infty dx \frac{1}{x} \frac{d\bar{n}}{dx}. \quad (8)$$

Using the transformation

$$R^2 [(k_j^2 - 1) \sin^2 \theta + 1] = Z_a^2 + k_j^2 x^2 \quad (9)$$

and differentiating Eq. (6), the angular deflection is given by

$$|\delta\phi(Z_a, t)| = \frac{4N_{Tj} k_j^3 Z_a K_j}{(v_{zj}^0 t)^4} \exp[-(Z_a/v_{zj}^0 t)^2]. \quad (10)$$

Differentiating with respect to time, the peak deflection will occur at the time t_{pj} given by

$$t_{pj} = \frac{Z_a}{\sqrt{2} v_{zj}^0}. \quad (11)$$

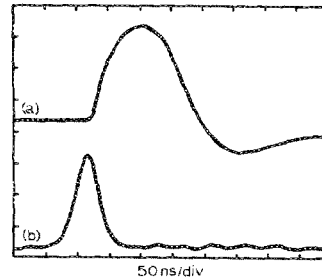


FIG. 4. (a) Position sensor output, 50 mV/div. Positive excursion is due to plasma, while negative excursion is due to neutral particles. Light attenuation is used to limit sensitivity of the sensor to 0.80 mV/ μ rad in this case. (b) PIN diode signal of the ruby laser pulse producing the plasma under investigation, 100 mV/div.

Hence, the expansion velocity for each species can be determined from the timing of the peak deflection due to that species, and using that velocity in Eq. (10), the number of each species produced by the laser is given by

$$N_{Tj} = |\delta\phi_{pj}| \left(\frac{\pi \exp(2)}{16}\right) \frac{Z_a^3}{K_j k_j^3} = 1.45 |\delta\phi_{pj}| \frac{Z_a^3}{K_j k_j^3}, \quad (12)$$

where $\delta\phi_{pj}$ is the peak angular deflection for each species.

An example of the experimental data is shown in Fig. 4. In this case, the orientation of the detector is such that the plasma electrons produce a positive deflection, while the neutral particles produce a negative deflection. (On shots where the ruby laser power fell below the threshold for plasma production, only the negative deflection was observed.) The detector was mounted 3.18 m from the target, and the detector sensitivity was calibrated at 4.0 mV/ μ rad; however, because of the large gradients involved, light attenuating filters were used in front of the detector to derate the sensitivity to 0.80 mV/ μ rad. For this particular shot, $Z_a = 0.192$ cm. One sees that the initial plasma peak is distinct from the later neutral peak, and that the plasma velocity is significantly higher than the neutral velocity. Using Eqs. (11) and (12), one finds that the characteristic velocities are $v_{zp}^0 = 3.0$ cm/ μ s and $v_{zn}^0 = 0.42$ cm/ μ s, while the number of particles produced by the laser are $N_{Tp} = 8.09 \times 10^{14}$, and $N_{Tn} = 3.76 \times 10^{16}$. The latter data correspond to peak densities along the path of the probe laser of $n_{pp} = 6.3 \times 10^{16}$ cm⁻³ and $n_{pn} = 7.3 \times 10^{17}$ cm⁻³ for the plasma and the neutral particles, respectively. These data are consistent with Faraday cup measurements of charged particles¹² and estimates of plasma density obtained spectroscopically as well as neutral particle density estimated from the size of the hole bored in the target by the ruby laser.¹

ACKNOWLEDGMENTS

This research was supported by NSF, ONR, and AFOSR. One of the authors (C.L.E.) was supported by AFIT/CIRD. The authors especially thank R. Spears for assistance in design and construction of the detector circuit.

¹M. L. Brake, J. S. Meachum, R. M. Gilgenbach, and W. Thornhill, IEEE Trans. Plasma Sci. PS-15, 73 (1987).

²R. H. Huddleston and S. L. Leonard, *Plasma Diagnostic Techniques* (Academic, New York, 1965).

³L. D. Horton and R. M. Gilgenbach, Phys. Fluids 25, 1702 (1982).

- ⁴M. Raleigh and J. R. Greig, NRL Memorandum Report No. 4390, February 1981.
- ⁵L. D. Horton and R. M. Gilgenbach, *Appl. Phys. Lett.* **43**, 1010 (1983).
- ⁶M. A. Greenspan and K. V. Reddy, *Appl. Phys. Lett.* **40**, 576 (1982).
- ⁷J. Pawliszyn, *Rev. Sci. Instrum.* **58**, 245 (1987).
- ⁸W. Lochte-Holtgreven, *Plasma Diagnostics* (North-Holland, Amsterdam, 1968), p. 190.
- ⁹I. A. D. Lewis and F. H. Wells, *Millimicrosecond Pulse Techniques* (McGraw-Hill, New York, 1954), p. 7.
- ¹⁰C. L. Enloe, Air Force Weapons Laboratory Report AFWL-TR-85-82, 1985.
- ¹¹G. J. Tallents, *Lasers Particle Beams* **1**, 171 (1983).
- ¹²J. S. Meachum, Ph.D. thesis, University of Michigan, 1987 (unpublished).